Journal of the Korean Physical Society, Vol. 50, No. 4, April 2007, pp. 1044∼1051

Sound Absorption of Micro-Perforated Panel

Sung Soo Jung,* Yong Tae Kim and Doo Hee Lee
Mechanical Metrology Group, Korea Research Institute of Standards and Science, Daejeon 305-340

Ho Chul Kim
Department of Physics, Korea Advanced Institute of Science and Technology, Daejeon 305-701

Seung Il Cho and Jong Kyu Lee
Department of Physics, Pukyong National University, Busan 608-737

(Received 5 December 2006)

Theoretical sound absorption coefficient and profile of micro-perforated single-, double-, and triple-layer systems with varying panel parameters were calculated by using the lumped and the distributed models for acoustic impedances. The sound absorption levels and profiles predicted by using the distributed model with Maa's acoustic impedance showed a close agreement for all panel systems with those obtained experimentally by using impedance-tube and reverberation-room tests.

PACS numbers: 43.55.Ev, 43.58.Bh
Keywords: Micro-perforated panel, Sound absorption coefficient, Impedance-tube test, Reverberation-room test

I. INTRODUCTION

Porous sound absorbent materials, such as glass wool, mineral wool, and urethane foam, produce unwanted floating dust particles in hospitals, infant facilities, dinning facilities, *etc.* Therefore, more environmentally-friendly sound absorption systems are required to upgrade hygienic condition without these hazardous sound absorbing materials. Sound absorption and damping are caused by the air flow resistance, and the resonance frequency is determined by the porosity, the number and the dimensions of the perforations, and the thickness of the air layer between the perforated panel and the backing plate. A micro-perforated sound absorbing panel resonance system is a substitutional method consisting of a large number of micro-sized Helmholtz resonator holes in front of an acoustically hard backing material.

The reflection and the transmission take place at the interface between the first and the second media, depending on the specific acoustic impedance of the second medium. The specific surface acoustic impedance (Z_s) is expressed in complex form as $Z_s = R_s + jX_s$, where R_s is the resistance and X_s is the reactance. The various acoustic impedance models proposed to account for the sound absorption in a micro-perforated panel are attributable to Maa [1], Beranek and Ver [2], and Rao and Munjal [3]. The sound absorption coefficient (α) defined by the ratio of the absorbed to the incident sound energy is given as $\alpha = 4R_s/[(1+R_s)^2 + X_s^2]$ for the case of normal incidence.

The theoretical sound absorption of a micro-perforated panel system has been investigated by using the lumped [1, 4] or the distributed models [5, 6] in terms of different acoustic impedances. Lee and Chen [5] and Lee and Kwon [6] compared the sound absorption coefficients calculated by using the lumped and the distributed models under limited experimental conditions.

In this work, we present the sound absorption coefficients as functions of frequencies calculated for single-, double-, and triple-perforated panels by using the lumped and the distributed models with three proposed acoustic impedances. The theoretically predicted profiles are compared with those obtained by using the impedance-tube and the reverberation-room tests to verify the sound absorption in the micro-perforated panel.

II. SPECIFIC ACOUSTIC IMPEDANCE OF A MIRCO-PERFORATED PANEL

A small hole in a micro-perforated panel, as shown in Figure 1, can be treated as a thin cylindrical tube. If the wave length of an incident wave (p_i) is long enough compared with the tube diameter and the distance between tubes, the specific acoustic impedance of the tube

*E-mail: jss@kriss.re.kr

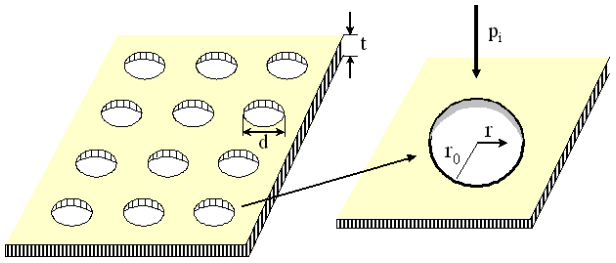

Fig. 1. Perforated panel.

is given as [7]

$$Z = j\omega\rho t\left[1 - \frac{2}{\xi\sqrt{-j}}\frac{J_1(\xi\sqrt{-j})}{J_0(\xi\sqrt{-j})}\right]^{-1}, \quad (1)$$

where ω is the angular frequency, ρ is the density of air, t is the thickness of the plate, r_0 is the hole radius, η is the dynamic viscosity constant of air, J_0 and J_1 are the Bessel functions of the first kind and the zeroth and the first order, respectively, $j = \sqrt{-1}$, and $\xi = r_o\sqrt{\rho\omega/\eta}$. The specific acoustic impedance of a perforated panel that contains many tubes can be obtained by dividing Eq. (1) by the porosity (p, the ratio of the perforated area to the area of the panel).

The specific acoustic impedance of Eq. (1) is inconvenient for the use in practice. Maa [1] proposed a more useful approximate solution with an error within 5 %, and the normalized specific impedance of the perforated panel, Z_{pM}, was given as

$$\begin{aligned} Z_{pM} &= Z/Z_0 = R_{pM} + jX_{pM}, \\ R_{pM} &= \frac{C_1 t\times 10^{-5}}{pd^2}\left(\sqrt{1+\frac{\chi^2}{32}} + \frac{\chi\sqrt{2}}{8}\frac{d}{t}\right), \\ X_{pM} &= 0.0185\frac{tf}{p}\left(1 + \frac{1}{\sqrt{9+\chi^2/2}} + 0.85\frac{d}{t}\right), \end{aligned} \quad (2)$$

where Z_0 is the acoustic impedance of air, R_{pM} and X_{pM} are the resistance and the reactance of the Z_{pM}, respectively, $\chi = C_2\times 10^{-3}d\sqrt{f}$, C_1 and C_2 are 0.147 and 0.316 for a non-metal plate and 0.335 and 0.21 for a metal plate, respectively, f is frequency, and d is the hole diameter. Beranek and Ver proposed a different form of the approximate resistance and reactance for the normalized specific acoustic impedance of a perforated panel [2]:

$$\begin{aligned} R_{pB} &= \frac{8.076\times 10^{-5}\sqrt{f}}{p}\left(1+\frac{t}{d}\right), \\ X_{pB} &= 0.0185\frac{f}{p}\left[\frac{0.0044}{\sqrt{f}}\left(1+\frac{t}{d}\right) + t + \delta\right], \end{aligned} \quad (3)$$

where $\delta = 0.85d\phi(p)$ is a function of the porosity and $\phi(p) = 1 - 1.47\sqrt{p} + 0.47\sqrt{p^3}$. The constant 0.85 in the reactance of Eqs. (2) and (3) corresponds to the end correction. On the other hand, Lee and Kwon [6] proposed another form of the resistance and the reactance based on Rao and Munjal's empirical model [3]:

$$\begin{aligned} R_{pL} &= 0.007337/p, \\ X_{pL} &= [2.89185\times 10^{-5}(1+51t)(1+204d)f]/p. \end{aligned} \quad (4)$$

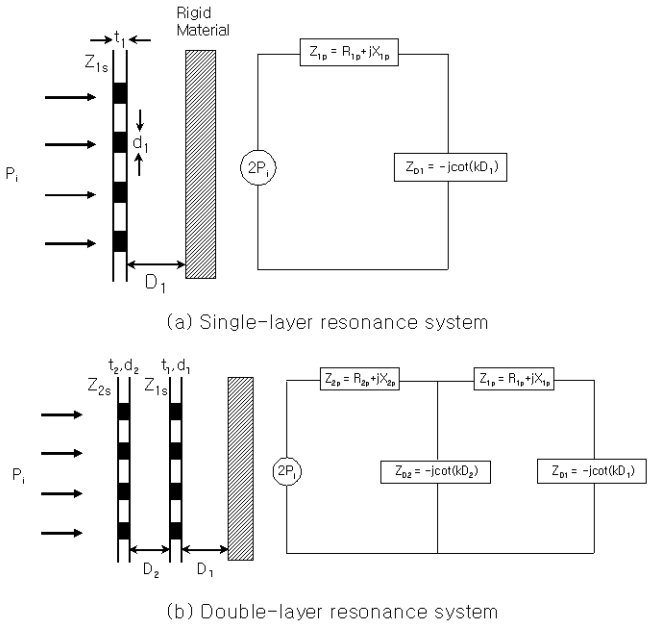

Fig. 2. Resonance sound absorption system and equivalent circuit analysis used for a lumped model: (a) single-layer system and (b) double-layer system.

III. THEORETCAL SOUND ABSORPTION COEFFICIENT OF THE MICRO-PERFORATED PANEL SYSTEM

A micro-perforated panel itself has a rather low sound absorption. However, the sound absorption drastically increases at the resonance frequencies if an air layer exist between the micro-perforated panel and the rigid backing material; such a system becomes a kind of resonance system as shown in Figure 2. Two analytical models, the shunt lumped and the distributed models analogous to an equivalent electric circuit, are available to account for the sound absorption characteristics.

1. Lumpted Model

The sound absorption of a micro-perforated panel system with a single-layer is shown in Figure 2(a). When a sound wave is incident normal to the micro-perforated panel, the acoustic impedance at the front surface is expressed as $Z_{1s} = R_{1p} + j[X_{1p} - \cot(kD_1)]$, where the reactance of air layer is $\cot(kD_1)$, k is the wave number, and D_1 is the air layer thickness. The resistance (R_{1p})

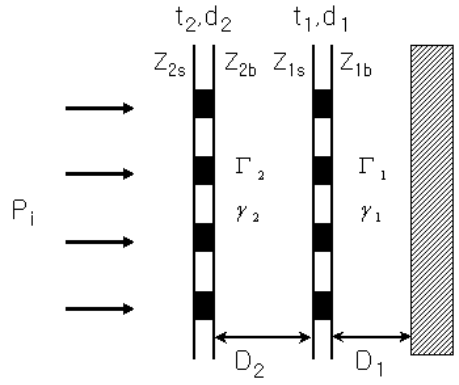

Fig. 3. Double-layer sound absorption system for a distributed model.

and the reactance (X_{1p}) of the micro-perforated panel are obtained by using Eq. (2) or (3) or (4), depending on the acoustic impedances chosen.

For the double-layer system shown in Figure 2(b), a second perforated panel having an acoustic impedance of $Z_{2p} = R_{2p}+jX_{2p}$ with an air thickness of D_2 is combined with the first panel. The surface acoustic impedance in front of the second panel is expressed as [4]

$$Z_{2s} = R_{2p} + jX_{2p} - \frac{j\cot(kD_2)[R_{1p} + j(X_{1p} - \cot(kD_1)]}{R_{1p} + j[X_{1p} - \cot(kD_2) - \cot(kD_1)]}. \quad (5)$$

The surface acoustic impedance in front of a triple-layer or more multi-layer system is calculated by using a similar procedure. The sound absorption coefficient of the single or multi-layer system is expressed as

$$\alpha_i = 1 - |(Z_{is} - 1)/(Z_{is} + 1)|^2, \quad (6)$$

where i represents the panel number ($i = 1$ for a single-layer system and $i = 3$ for a triple-layer system).

2. Distributed Model

A double-layer resonance system is modeled as shown in Figure 3. The characteristic impedance and the propagation constant of the first and the second layers were represented as Γ and γ with subscript 1 and 2, respectively. The acoustic impedance behind the first perforated panel, Γ_{1b}, is expressed in general form as [8]

$$\Gamma_{1b} = \Gamma_1 \frac{Z_r \cosh(\gamma_1 D_1) + \Gamma_1 \sinh(\gamma_1 D_1)}{Z_r \sinh(\gamma_1 D_1) + \Gamma_1 \cosh(\gamma_1 D_1)}, \quad (7)$$

where Z_r is the acoustic impedance behind the first material and is assumed to be infinity for rigid material.

When the first material is air, Γ_{1b} is equal to $-j\cot(kD_1)$ for a rigid backing material. The surface acoustic impedance of the first perforated panel is the sum of the first perforated panel impedance itself (Z_{1p}) and Γ_{1b} expressed as $Z_{1s} = Z_{1p} + \Gamma_{1b} = R_{1p} + j[X_{1p} - \cot(kD_1)]$, which is the same form as that of the lumped model. For a double-layer system, the acoustic impedance behind the second perforated panel, Γ_{2b}, is obtained by substituting Z_{1s}, Γ_2, γ_2, and D_2 for Z_r, Γ_1, γ_1, and D_1 in Eq. (7):

$$\Gamma_{2b} = \Gamma_2 \frac{Z_{1s} \cosh(\gamma_2 D_2) + \Gamma_2 \sinh(\gamma_2 D_2)}{Z_{1s} \sinh(\gamma_2 D_2) + \Gamma_2 \cosh(\gamma_2 D_2)}. \quad (8)$$

Then, the surface acoustic impedance in front of the second panel is expressed as

$$Z_{2s} = Z_{2p} + \Gamma_{2b}. \quad (9)$$

By using a similar procedure, the surface acoustic impedance in front of a triple-layer or more multi-layer system can be calculated by substituting the appropriate γ, D, and Γ. The sound absorption coefficients are obtained by using Eq. (6) and substituting the appropriate surface impedance. The basic difference between the lumped and the distributed models is that the former assumes the back surface acoustic impedance of the air layer to be that of a rigid material whereas the latter assumes the surface impedance of the last micro-perforated plate. The sound absorption coefficients for a single-layer system calculated by using the lumped and the distributed models are the same, $Z_{1s} = R_{1p} + j[X_{1p} - \cot(kD_1)]$, but they are different for a multi-layer system.

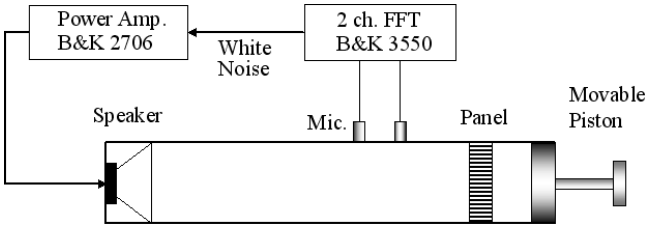

Fig. 4. Schematic diagram of the impedance-tube test method.

IV. EXPERIMENTS

1. Impedance-tube Test

A schematic diagram of the impedance-tube test is shown in Figure 4. The hole diameter of the perforated panel is 100 mm. White noise was generated up to 1600 Hz by using a frequency analyzer (B&K 3550) and was amplified with a power amplifier (B&K 2706). Two 1/4-inch microphones (B&K 4187) were flush mounted at the surface of the impedance-tube, and the magnitude and the phase mismatch were corrected by using the sensor switching method. The sound absorption coefficients were obtained by using the two-microphone method [9].

Figure 5 presents the profiles of the sound absorption coefficients of a single-layer micro-perforated panel having the panel parameters $t_1 = d_1 = 1$ mm, $p_1 = 1$ %,

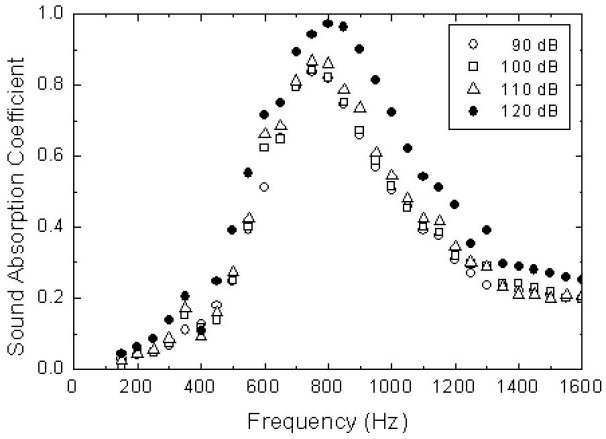

Fig. 5. Comparison between the measured sound absorption coefficients of a single-layer micro-perforated panel with $t_1 = d_1 = 1$ mm, $p_1 = 1$ %, and $D_1 = 30$ mm for various the generated sound pressure levels inside the impedance tube.

and $D_1 = 30$ mm at various sound pressure levels in the impedance tube. The profiles of the sound absorption under 110 dB show a consistent pattern. However, the profile at a sound pressure of 120 dB was broadened with a greater maximum sound absorption, and the resonance frequency shifted toward higher frequency due to the excessive sound pressure in the impedance tube. All the proceeding measurements of sound absorption in the impedance tube were conducted while keeping the sound pressure level under 100 dB.

2. Reverberation-room Test

When the sound is obliquely incident at an angle θ as shown in Figure 6, the air layer is partitioned by means of a structure, often called locally the reacting boundary. The sound absorption coefficient [8] is expressed with a total surface acoustic impedance ($Z_t = R_t + jX_t$) as

$$\alpha(\theta) = \frac{4R_t \cos\theta}{[R_t \cos\theta + 1]^2 + [X_t \cos\theta]^2}. \tag{10}$$

The statistical sound absorption coefficient in a diffuse sound field can be expressed as

$$\alpha = 2\int_0^{\pi/2} \alpha(\theta)\cos\theta \sin\theta d\theta. \tag{11}$$

The sound absorption coefficients of a single-layer micro-perforated panel with a total surface area of 10 m^2 was measured in a reverberation room at the center frequency of the 1/3-octave band according to ISO 354 [10], as shown in Figure 7. In order to achieve a locally reacting condition as shown in Figure 6, we used a honeycomb structure behind the micro-perforated panel.

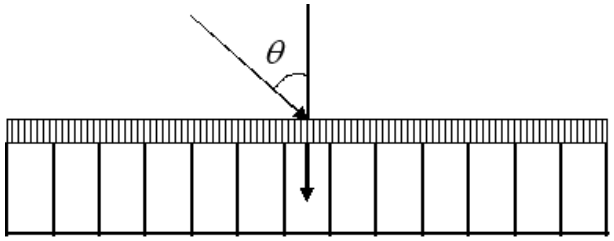

Fig. 6. Air layer as partitioned by the structure.

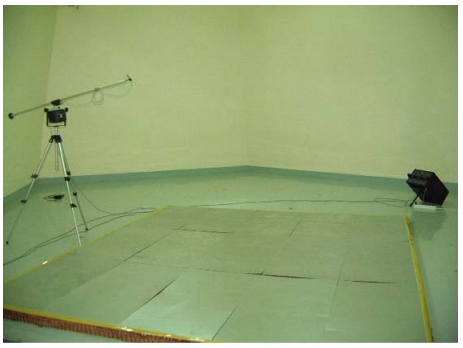

Fig. 7. Sound absorption test in an anechoic room.

V. RESULTS AND DISCUSSION

1. Sound Absorption Coefficients of a Single-layer Panel

A. Theoretical Sound Absorption Coefficients with Various Acoustic Impedances

The theoretical sound absorption coefficients of the micro-perforated panel were calculated by using the distributed model and substituting respective normal acoustic impedances of Eq. (2) by Maa [1], Eq. (3) by Beranek and Ver [2], and Eq. (4) by Lee and Kwon [6] and are compared in Figure 8. The panel parameters used in the calculation are $t_1 = 0.5$ mm, $d_1 = 1$ mm, $p_1 = 1$ %, and $D_1 = 30$ mm in Figure 8(a). Both Maa's and Beranek and Ver's acoustic impedance models yielded similar sound absorption profiles with an absorption peak of 0.75 at 800 Hz whereas Lee and Kwon's model yielded a greater maximum sound absorption coefficient at around 700 Hz, a lower frequency.

The sound absorption profiles calculated by using the distributed model changed markedly as the panel thickness was increased from $t_1 = 0.5$ mm to 10 mm, as seen in Figure 8(b). The levels of the sound absorption coefficients are similar, but the resonant frequencies of Maa and Beranek and Ver are shifted to a lower frequency of 270 Hz from 800 Hz whereas that of Lee and Kwon is shifted to 580 Hz from 700 Hz. The results indicate that we are not in position yet to determine the appropriate impedance.

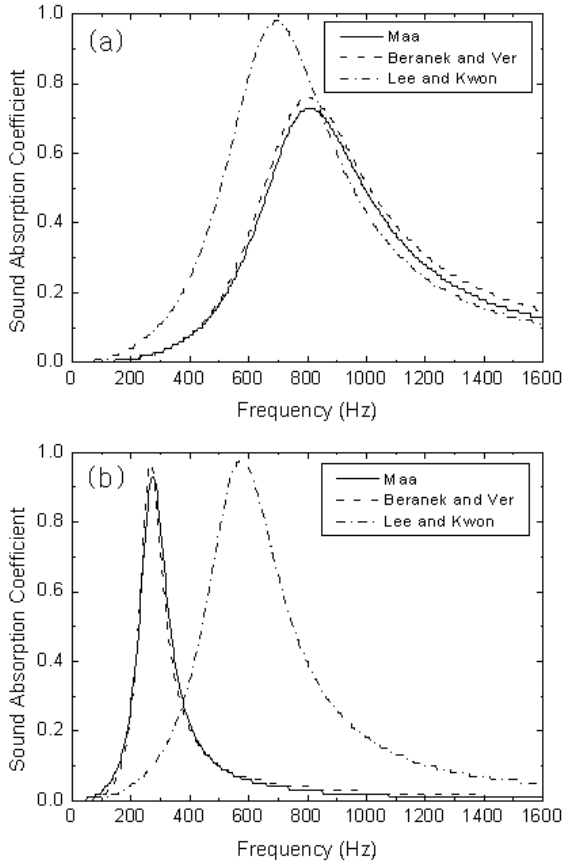

Fig. 8. Comparison between the simulated sound absorption coefficients of a single-layer system by using Maa's, Beranek and Ver's, and Lee and Kwon's acoustic impedances: (a) panel parameters $t_1 = 0.5$ mm, $d_1 = 1$ mm, $p_1 = 1$ %, and $D_1 = 30$ mm and (b) panel parameters $t_1 = 10$ mm, $d_1 = 1$ mm, $p_1 = 1$ %, and $D_1 = 30$ mm

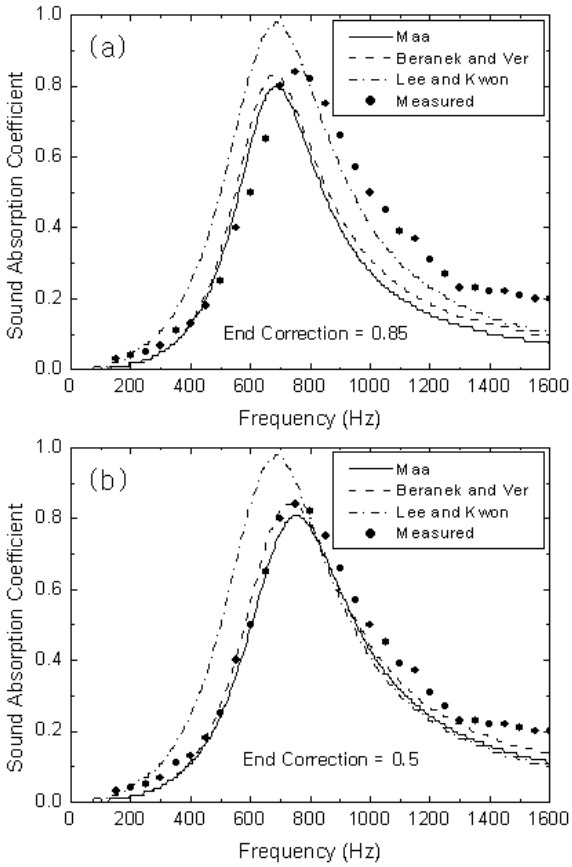

Fig. 9. Comparison between the measured and the calculated sound absorption coefficients of a single-layer system by using Maa's, Beranek and Ver's, and Lee and Kwon's acoustic impedance for the panel parameters $t_1 = d_1 = 1$ mm, $p_1 = 1$ %, and $D_1 = 30$ mm: (a) the end correction=0.85 and (b) the end correction=0.5.

B. Comparison of the Theoretical Predictions with the Impedance-tube Results

The sound absorption coefficients of a single-layer panel with the same panel parameters of $t_1 = d_1 = 1$ mm, $p_1 = 1$ %, and $D_1 = 30$ mm were calculated for each acoustic impedance. The sound absorption profiles were compared in Figures 9(a) and (b) with the values measured by using the impedance tube. They do not agree well; the measured profiles are broader, and the resonance is at a higher frequency. To account for the disagreement, the end correction in the acoustic impedance of the theoretical prediction was changed from 0.85 to 0.5 as proposed by Dean [11]. The sound absorption profiles with the 0.5 end correction of Maa's and Beranek and Ver's acoustic impedances exhibit the closest agreement with the experimental profiles obtained by using the impedance tube in the aspect of the level of maximum absorption at 750 Hz, as shown in Figure 9(b).

C. Reverberation-room Test

When the perforated panel is thin enough, the resonance due to a panel bending motion and damping factor should be considered [12,13]. In order to check the panel bending motion, the velocity of the perforated panel was measured by using an accelerometer (B&K 4370) with a charge amplifier (B&K 2635) and was analyzed with a dynamic signal analyzer (H.P. 35670A), as shown in Figure 10, and no noticeable velocity change due to the panel resonance was observed. The velocity decreased with frequency monotonously, indicating no bending motion of the plate.

Figure 11 is a comparison of the measured values and the theoretical profiles obtained by using Eq. (11) with Maa's acoustic impedance with an end correction factor of 0.5 for a single-layer panel ($t_1 = 0.5$ mm, $d_1 = 1$ mm, $p_1 = 1.2$ %, and $D_1 = 20$ mm), and the agreement is very satisfactory. The comparison between the measured and

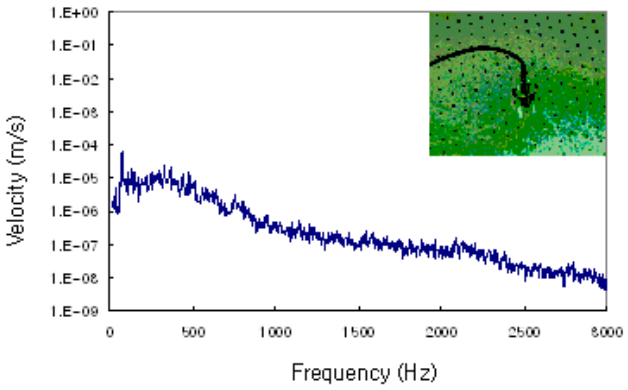

Fig. 10. Vibration velocity measured on the micro-perforated panel.

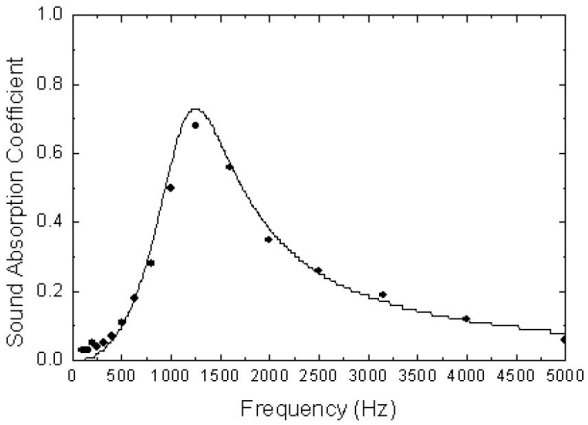

Fig. 11. Comparison between the measured sound absorption coefficients of a single-layer panel with the panel parameters $t_1 = 0.5$ mm, $d_1 = 1$ mm, $p_1 = 1.2$ %, and $D_1 = 20$ mm by using the reverberation room test and those theoretically calculated by using the distributed model with Maa's acoustic impedance and an end correction factor of 0.5.

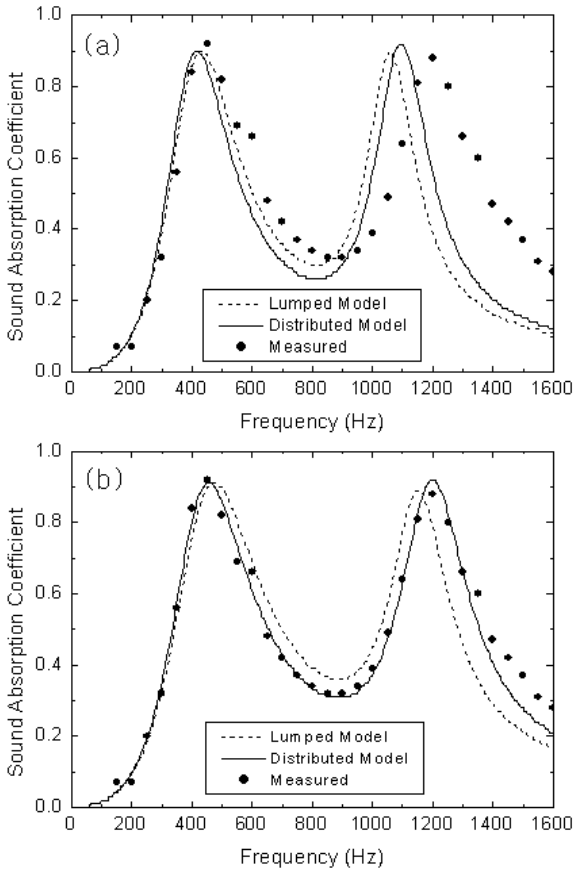

Fig. 12. Comparison between the measured sound absorption coefficients of a double-layer panel and the theoretical values calculated by using the lumped and the distributed models with Maa's acoustic impedance and different end corrections: (a) the end correction = 0.85 and (b) the end correction = 0.5.

the calculated sound absorption coefficients indicate that both Maa's and Beranek and Ver's impedances are more effective than Lee and Kwon's impedance.

2. Sound Absorption Coefficients of Double- and Triple-layer Panels

A. Comparison with the Results in the Impedance-tube Test

Theoretical sound absorption coefficients calculated by using the lumped and the distributed models with Maa's acoustic impedance for a double-layer panel with the panel parameters $t_1 = t_2 = d_1 = d_2 = 1$ mm, $p_1 = p_2 = 1$ %, and $D_1 = D_2 = 30$ mm are presented in Figures 12(a) and (b) with correction factors of 0.85 and 0.5, respectively. The profile calculated by using the distributed model with Maa's acoustic impedance and an end correction of 0.5 shows a better agreement with the measured values, as shown in Figure 12(b). The two sound absorption coefficient maxima, one at 450 and the other at 1200 Hz, correspond to those at each layer in the double-layer panel.

The sound absorption coefficients of a double-layer panel calculated by using the distributed model with the acoustic impedances of Maa and Beranek and Ver are compared with the values measured in the impedance tube in Figure 13 for the same panel parameters as those in Figure 12(b). Maa's acoustic impedance is shown to be more effective than Beranek and Ver's with respect to the levels of the sound absorption coefficients and the resonance frequencies.

Figure 14 shows the profiles of the theoretical sound absorption coefficients calculated by using the distributed model with Maa's acoustic impedance and the values measured for a triple-layer system with the parameters $t_1 = t_2 = t_3 = d_1 = d_2 = d_3 = 1$ mm, $p_1 = p_2 = p_3 = 1$ %, $D_1 = 50$ mm, and $D_2 = D_3 = 30$ mm. Three ab-

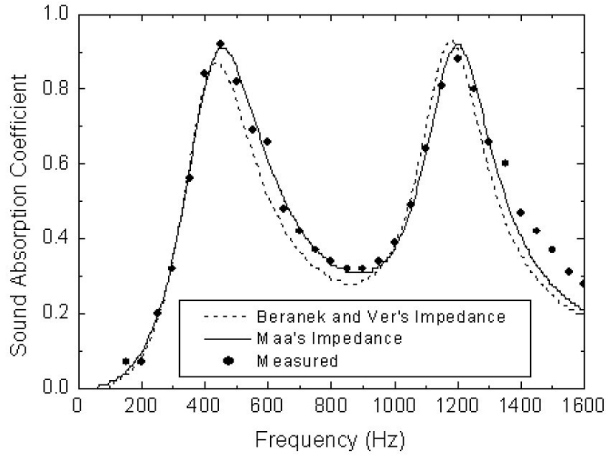

Fig. 13. Comparison between the measured sound absorption coefficients of a double-layer system and the theoretical values calculated by using the distributed model with Maa's and Beranek and Ver's acoustic impedances and an end correction of 0.5.

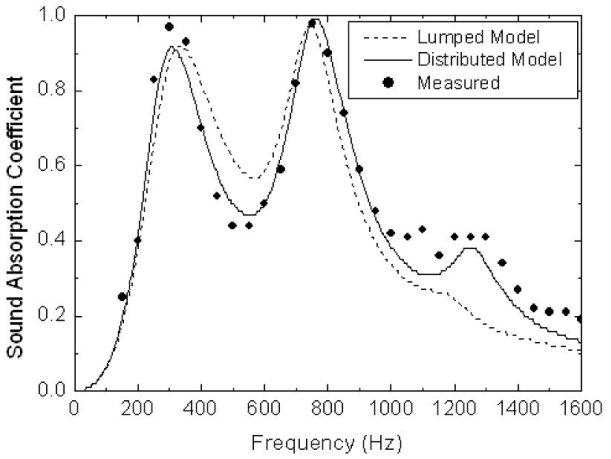

Fig. 14. Comparison of the measured sound absorption coefficients of a triple-layer system with the theoretical values calculated by using two different models with Maa's acoustic impedance and an end correction factor of 0.5.

sorption peaks are observed, 300, 750, and 1250 Hz, corresponding to each layer of the triple-layer panels. Maa's acoustic impedance with an end correction factor of 0.5 agrees well with the measured profiles of the three absorption maxima at the resonant peak frequencies. Now, we can conclude that the sound absorption coefficients calculated by the distributed model with Maa's acoustic impedance show closest agreement with those measured in the impedance tube for a micro-perforated panel system.

B. Reverberation-room Test

In Figures 15(a) and (b), the profiles of the sound absorption coefficients calculated theoretically by using the

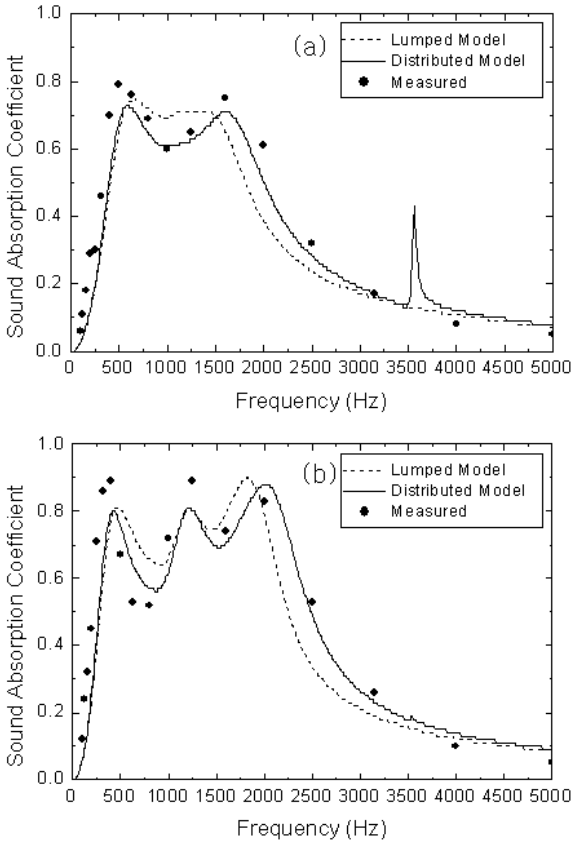

Fig. 15. Comparison between the measured sound absorption coefficients of a doulbe-layer and a triple-layer system and the theoretical values calculated by using two different analyses with Maa's acoustic impedance and an end correction factor of 0.5: (a) double-layer system and (b) triple-layer system.

lumped and the distributed models for a double-layer and a tirple-layer panel system are compared with those measured in the reverberation room. The parameters involved for the double-layer system were $t_1 = 0.5$ mm, $d_1 = 1.5$ mm, $p_1 = 2.5$ %, $D_1 = 25$ mm, $t_2 = 0.5$ mm, $d_2 = 1$ mm, $p_2 = 1$ %, and $D_2 = 50$ mm; for the triple-layer system, they were $t_1 = 0.5$ mm, $d_1 = 1.5$ mm, $p_1 = 2.5$ %, $D_1 = 20$ mm, $t_2 = 0.5$mm, $d_2 = 1$ mm, $p_2 = 1.2$ %, $D_2 = 25$ mm, $t_3 = 0.5$ mm, $d_3 = 1.5$ mm, $p_3 = 1$ %, and $D_3 = 50$ mm. The results again confirm that the sound absorption coefficients of the double- and the triple-layer panels can be described adequately by the distributed model with Maa's acoustic impedance, regardless of the panel parameters.

VI. CONCLUSION

The sound absorption coefficient of layer panel varied markedly with the acoustic impedance and sound pres-

sure. Theoretical sound absorption coefficient calculated by using the distributed models of a single-layer for the same panel parameter by using acoustic impedances of Maa and Beranek and Ver yielded an absorption peak of 0.75 at 800 Hz, whereas Lee and Kwon's model yielded a greater maxima sound absorption coefficient at the lower frequency of around 700 Hz. The sound absorption profiles of the panel also changed significantly in aspect of the resonance frequency with increasing the panel thickness, shifting to the lower frequency. The theoretical prediction and impedance-tube test results agreed well by introducing the end correction factor of 0.5. Two and three peaks observed in the absorption profile corresponding to the double-layer and the triple-layer systems, respectively are in good argeement with those predicted by the distributed model with Maa's acoustic impedance of the end correction of 0.5.

REFERENCES

[1] D. Y. Maa, Scientia Sinica **18**, 55 (1975).

[2] L. L. Beranek and I. L. Ver, *Noise and Vibration Control Engineering* (John Wiley and Sons, New York, 1992), Chap. 8.

[3] K. N. Rao and M. L. Munjal, J. Sound Vib. **108**, 283 (1986).

[4] J. Kang and H. V. Fuchs, J. Sound Vib. **220**, 905 (1999).

[5] F.-C. Lee and W.-H. Chen, J. Sound Vib. **248**, 621 (2001).

[6] D. H. Lee and Y. P. Kwon, J. Sound Vib. **278**, 847 (2004).

[7] I. B. Crandall, *Theory of Vibrating Systems and Sound* (Van Nostrand, New York, 1926), p. 229.

[8] K. U. Ingard, *Notes on Sound Absorption Technology* (Noise Control Foundation, New York, 1994), Chap. 1.

[9] J. Y. Chung and D. A. Blaser, J. Acoust. Soc. Am. **68**, 907 (1980).

[10] ISO 354 Acoustics-Measurement of sound absorption in a reverberation room (2003).

[11] L. W. Dean, NASA Rept. CR-134912, PWA-5311, 1976.

[12] Y. Y. Lee, E. W. M. Lee and C. F. Ng, J. Sound Vib. **287**, 227 (2005).

[13] S. S. Jung, Y. T. Kim, Y. B. Lee, S. H. Shin, D. Kim and H. C. Kim, J. Korean Phys. Soc. **49**, 1961 (2006).